Synsint Research Group

Available online at www.synsint.com

Synthesis and Sintering

ISSN 2564-0186 (Print), **ISSN** 2564-0194 (Online)

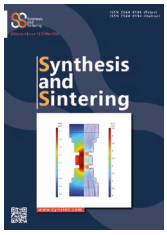

Research article

Effects of cerium oxide and cerium sulfate on the optical behavior of synthesized garnet glass ceramics

A. Faeghinia

Department of Ceramics, Materials and Energy Research Center, Karaj, Iran

ABSTRACT

In this study, YAG silicate glasses were prepared by incorporating cerium sulfate and cerium oxide salts (composition: $17YO_3$-$33Al_2O_3$-$40SiO_2$-$2AlF_3$-$3NaF$-$2CeO_2$-$3B_2O_3$) using the melting method. Subsequently, glass ceramics were obtained through heat treatment of the base glasses. According to the photoluminescence spectra of both glasses, emissions were observed at wavelengths of 466 nm and 435 nm, attributed to cerium ions. It was shown that the garnet crystals formed less during the heat treatment process in the sample containing cerium sulfate compared to the sample with cerium oxide. The emission spectra of both glass-ceramics, when excited at 240 nm, fall within the wavelength range of 460 nm. Also, emissions at wavelengths of 534 nm and 660 nm were observed under excitation at 340 nm. Heat treatments were conducted using three methods: in an oxide atmosphere using a tubular furnace (single-step), via spark plasma sintering (SPS) of powder, and in a hydrogen atmosphere (with two-steps heating). According to the XRD results, the entry of cerium into the garnet structure was affected by the heat treatment duration of 24 h and the temperature of 1060 °C. Finally, by comparing the spectroscopic results, it was found that the optical response of the garnet glass-ceramic synthesized in the hydrogen atmosphere occurred at a wavelength of 400 nm, suggesting its potential application in the LED industry.

KEYWORDS

YAG
Glass ceramic
Luminescence
Cerium
Spark plasma sintering
Synthesis

OPEN ACCESS

1. Introduction

Advancements in materials science will undoubtedly be constrained by the scarcity of available data on the microstructure of materials. Analyzing the structure of materials characterized by long-range crystal order is a routine procedure [1]. White diode lamps are a new generation of solid-state lighting fixtures that have become normal in our daily lives. Previously, Ce:$Y_3Al_5O_{12}$ glass ceramics have been suggested as phosphorescent materials. Since Ce:YAG microcrystals are deposited within the glass substrate by surface crystallization mechanism, they exhibit superior at high temperature and humidity conditions compared to traditional commercial LEDs [2–5].

In commercial LEDs, phosphorescent materials are typically injected into the resin matrix. However, in Ce:YAG-GC, Ce^{3+} ions are deposited within the Y sites of Ce:YAG microcrystals. These ions emit yellow fluorescent light when optically stimulated by a blue LED [6]. Hence, the final white light emission can be obtained by combining blue excitation light and yellow fluorescence light [7]. The preparation of Ce:YAG glasses presents challenges owing to their high melting point. Additionally, the process of preparing glass-ceramics is particularly complicated due to the elevated alumina content. Various efforts have been made to solve this issue, such as incorporating silica into the composition of YAG glass [8, 9]. Based on previous research, the amounts of silica and alkalis in the primary glass composition should ideally remain below 40 mol%. Exceeding this threshold may lead to the crystallization of the YAS phase within the system, thereby decreasing the crystallization of the YAG garnet phase. Since the garnet phase is a suitable host for rare earth ions, its formation in the

* Corresponding author. *E-mail address:*a.faeghinia@merc.ac.ir (A. Faeghinia)
Received 1 November 2023; Received in revised form 23 February 2024; Accepted 24 February 2024.

https://doi.org/10.53063/synsint.2024.41186

glass phase is important. On the other hand, the formation of YAS phase in the glass system reduces the reflective properties of the glass [10].

On the other hand, cerium ions can exist in the glass melt in two oxidation states 3 and 4. By heat treatment, Ce^{3+} ion (cerous ion) enters the structure of garnet and is replaced with yttria ion, which exhibits luminescent properties as a result of crystal splitting [11]. The study examining the effect of cerium doping on the microstructure and performance of Al_2O_3–Ce:YAG composite ceramics, fabricated by reactive vacuum sintering, recognized the optimal cerium concentration for enhancing phosphor efficiency. Results showed that higher cerium amounts partially recharge the composites and introduce magnesium ions, improving crystal structure stability. Optimal photoluminescence intensity was observed in the 0.1 at% Ce^{3+} sample. The ceramic phosphors displayed a minimal reduction in photoluminescence emission intensities at high temperatures and showed promising applicability for natural white light-emitting diodes that offer a balance between color quality and luminous efficiency [12].

A facile route for synthesizing YAG nanophosphors via a Pechini-type sol-gel process for white light-emitting diode (LED) technology is described. The wet-type synthesis was followed by a heat treatment at 1000 °C for 4 h. A study of the luminescent properties of the YAG:Ce,Pr system was carried out, with the concentration of praseodymium varied while maintaining the quantity of cerium constant. The purity of the YAG phase was confirmed by diffractometric analysis. Luminescent analysis revealed the typical Ce^{3+} emission overlapped with sharper Pr^{3+} emissions in the red region of the spectrum. The presence of the energy transfer phenomenon was confirmed by the photoluminescence excitation (PLE) spectra of the samples, with concentration quenching observed at 0.5 mol% Pr resulting in a decrease in both the intensity of praseodymium emission and mean lifetime [13].

In the series of research, the flame method with a fast cooling rate was used to prepare YAS glass ceramic. The glass-forming ability in the YAS system is highly dependent on the amount of silica. In the flame spray method, the complete combustion of acetylene causes a temperature above 3200 °C, during melting, the glass particles are cooled in water, this rapid cooling leads to the creation of YAS with a low amount of silica [14, 15].

In the solid-state synthesis of garnet, heat treatment is carried out in a reducing atmosphere to encourage the cerium ions formation. However, in the preparation of YAG glass melt, there is no mention of the atmosphere in the melting environment, and no comparison has been made regarding the influence of different heat treatment atmospheres. Since the oxidation amount of cerium in glass and glass-ceramic garnet is important, therefore assuming that changing the supply source can have a role in the oxidation number of cerium, in the present work by changing the supply source of cerium (sulfate type and oxide type) in glass melt, an attempt was made to investigate the behavior of cerium ion in glass and glass-ceramic indirectly by measuring the optical properties of the fabricated glass and glass-ceramic. Also, with the assumption that the use of SPS for the heat treatment of YAG glass can create simultaneous reduction conditions with pressure, so this method was also used for glass powder sintering and simultaneous heat treatment for crystallization [16, 17].

The purpose of this research is to explore a suitable synthesis approach for YAG silicate glasses using cerium sulfate and cerium oxide salts. By investigating the effects of different salt types and heat treatment conditions, valuable insights are gained into optimizing the fabrication process for YAG-based materials.

2. Experimental procedure

Raw materials were prepared from Aldrich company with the following specifications: CAS Number: 7784-18-1 AlF_3, CAS Number: 1344-28-1 Al_2O_3, CAS Number: 7681-49-4 NaF, CAS Number: 1314-36-9 Y_2O_3, CAS Number: 1306-38-3 CeO_2, CAS Number: 10043-35-3 H_3BO_3.

Acid-washed silica was extracted from the Azandarian Mine in the Hamedan province of Iran, while double hydroxide cerium sulfate was derived from locally sourced monazite mineral through a precipitation method for separating cerium from nuclear reactor waste and concentrate. It's worth noting that the cerium extraction process also involved neodymium and yttria impurities at a concentration of 1000 ppm. Fig. 1 depicts the XRD pattern of the amorphous cerium sulfate, the XRD pattern of the sample containing cerium oxide, the appearance of glass samples poured with cerium sulfate and cerium oxide, and the temperature-time curve for the SPS sample, respectively. As seen, the gel deposit, cerium sulfate, is amorphous and possesses a weak crystal structure. The composition used to prepare YAG glass was prepared using cerium oxide and cerium sulfate ($17YO_3$-$33Al_2O_3$-$40SiO_2$-$2AlF_3$-3NaF-$2CeO_2$-$3B_2O_3$) in terms of molar percentage.

The glass batch, weighing 10 grams, was melted twice at 1580 °C using an electric furnace. Finally, yellow glass was formed. Assuming the removal of sulfates from the molten glass system, calculations were performed to estimate the creation of 2 and 1 mol% cerium oxide in the glass following the decomposition of cerium sulfate. Subsequently, glasses containing sulfates were denoted as IK2 and IK1, while the cerium oxide-bearing glass was labeled CeO_2.

The spark plasma sintering equipment utilized in this study was manufactured by Easy Fashion Company in China This device has a maximum output current of 10 kA and a maximum power of 100 kW. The glass powder from the IK1 and IK2 samples was mixed in nearly equal proportions to facilitate the formation of a transparent glass phase using the SPS method. Subsequently, the sintered samples were successfully achieved in a transparent and glassy form.

The heating profile for the SPS furnace is as follows: Initially, the temperature is raised to 600 °C at a current of 0.7 amps, maintained for 5 minutes. Subsequently, the temperature is further increased to 1080 °C and held constant for an additional 5 minutes before the sample is removed. Fig. 1d shows the time-temperature curve for the SPS process.

2.1. Thermal analysis

To investigate the thermal behavior of each glass sample, the glass transition temperature (T_g), and crystallization peak temperature (T_x) were determined using thermal analysis (DTA). For this purpose, the glass was crushed and passed through the sieve with 30 mesh, then the glass on the sieve with 40 mesh was used in the amount of 1 g for DTA analysis. The reference material utilized for the mentioned device is α-alumina. The temperature increase rate within the device is set at 10 °C/min, reaching a final test temperature of 1200 °C. The simultaneous thermal analysis test was performed using a device (STA 503 made by BAHR, Germany). This device can achieve a maximum temperature of 1200 °C, with heating occurring at a rate of 10 °C/min.

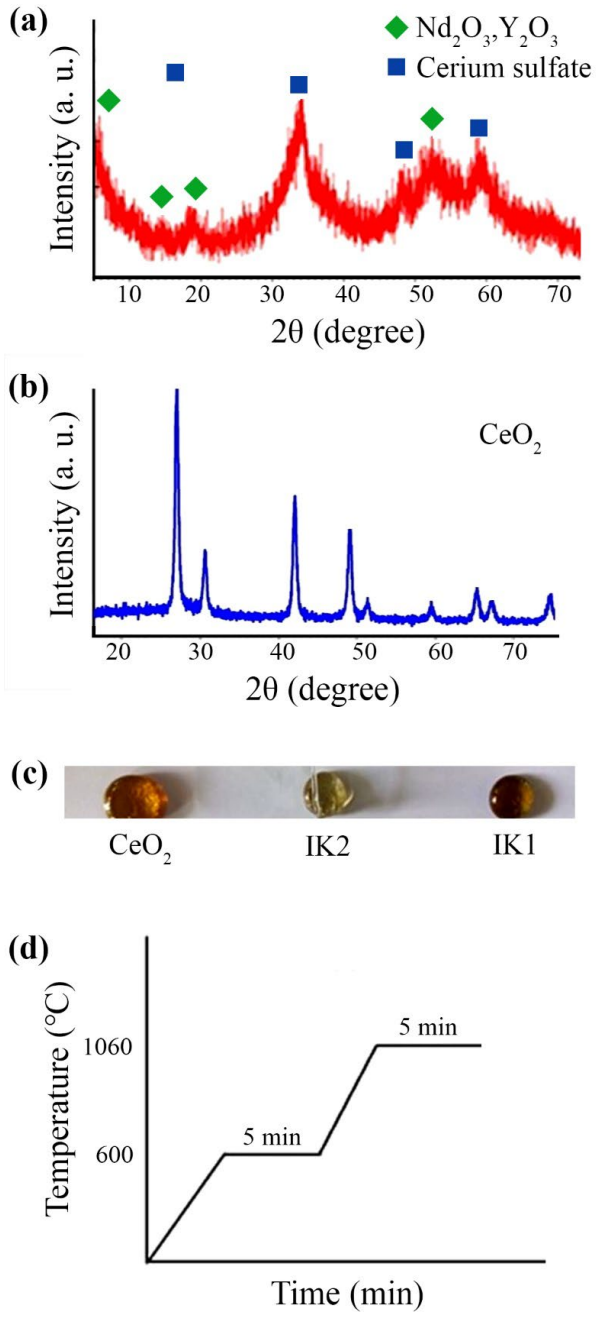

Fig. 1. a) XRD pattern of amorphous sulfate cerium, b) XRD pattern of oxide cerium, c) cast glasses treated with cerium oxide and cerium sulfate, and d) the stages involved in the SPS process.

Additionally, alumina powder and an air atmosphere were utilized as reference materials.

2.2. UV-Vis absorption spectrum

Perkin Elmer-lambada 25 visible-ultraviolet spectrometer was used to check the transparency, and absorption spectrum. To prepare the surface of the samples to be smooth and polished, they were sanded with 2500 abrasive. The rationale behind utilizing ultraviolet-visible measurement was the convenience and accessibility of the corresponding device in comparison to alternative analytical methods [18].

2.3. FTIR structural analysis

FT-IR analysis was used to determine the structure and arrangement of different groups of glasses. An infrared spectrometer analysis device model spectrum 400 made by PERKIN ELMER was used. In FTIR analysis, a specific amount of powder is mixed with KBr powder at a ratio of 1:100 by weight. The mixture is then compressed into a tablet to assess the absorption of the target substance within the IR spectrum. The choice of KBr is due to its minimal absorption in the target wavelength region. Therefore, it is possible to obtain the complete absorption spectrum of the unknown sample. The glass powder grains used in this analysis were finely sized and sieved through a 200-mesh sieve.

2.4. Spectrum of light emission

The samples of glass and glass-ceramic containing cerium were analyzed using the Perkin-Elmer LS-5 device, equipped with a xenon lamp, to investigate emission wavelengths within the range of 240–700 nm.

2.5. X-ray analysis

X-ray diffraction analysis was utilized to investigate the phases formed before and after heat treatment. The analysis was conducted using a Philips PW 3710 device with a Cu-Kα wavelength of 0.1542 nm. The examination covered a range of 2θ=10–80 °, employing an accelerating voltage of 40 kV and a current intensity of 30 mA. The measurement was performed with a step size of 0.20 ° and a step time of 2 °. X'Pert HighScore Plus software (version 5.1) was employed to identify the phases.

3. Results and discussion

3.1. Absorption of YAG glasses containing cerium oxide and cerium sulfate

To compare the physical properties and light absorption characteristics in both the visible and ultraviolet regions of glasses derived from cerium sulfate and cerium oxide, an optical absorption test was conducted. The results of this test are depicted in Figs. 2 and 3.

Fig. 2. shows the ultraviolet (UV) absorption spectrum of YAG glass formulation with cerium oxide. As observed, light transmission occurs in these glasses at wavelengths higher than 433 nm, making the glass transparent beyond this wavelength. The glasses exhibit a color spectrum ranging from yellow to orange. According to previous research [2, 13, 19], silica glass doped with ceria at a concentration of less than 6.5 mol% is colorless and exhibits maximum absorption at a wavelength of 320 nm. The intensity of absorption increases with increasing ceria content. When glass is melted in an oxygen-rich environment, its ultraviolet (UV) absorption increases within the range of 200–320 nm. It is clear that in cerium containing YAG glass, absorption in the wavelength range of 260 nm occurs due to the presence of a small amount of ceric ions (4+) in addition to cerous ions (3+) in the glass. In glasses containing cerous ions (3+), they act as electron donors and ceric ions act as electron acceptors (traps) [20–22].

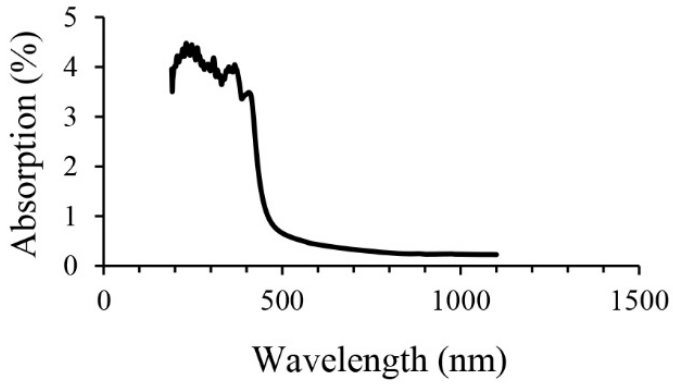

Fig. 2. The UV-Vis absorption spectrum of YAG composition on the base of cerium oxide.

Therefore, ceric ions stabilize the glass against discoloration. The stabilization of the partial yellow color in the present glasses is due to the extension of the absorption band of ceric ions into the visible range. The absorption peak of ceric ions is at the wavelength of 260 nm, and the absorption of ceric ions is much stronger than that of cerous ions in the UV range. Ceric ions possess a 4F electron configuration, and their adsorption is attributed to charge transfer phenomena. It is clear that silica glass primarily contains cerous ions, with minimal presence of ceric ions. The ultraviolet absorption of ceric ions is usually completely covered by the ultraviolet absorption limit of most glasses [23].

The absorption results of the UV range in the IK1 glass sample are shown in Fig. 3a. Clear absorption peaks ranging from 500 to 800 nm have appeared, attributed to the presence of impurities, specifically other rare earth elements in ppm, as detailed in the raw materials section. However, these minor impurities also cause light absorption in the glass. By referring to the articles, the origin of these peaks is determined. In phosphate and borate-base glasses, it has been proven that neodymium ion has the main absorption peak at wavelengths 584, 745, and 806 nm. Each of these peaks signifies energy transfer within the sublayers of the Nd^{3+} ion [24]. These distinct absorption peaks were

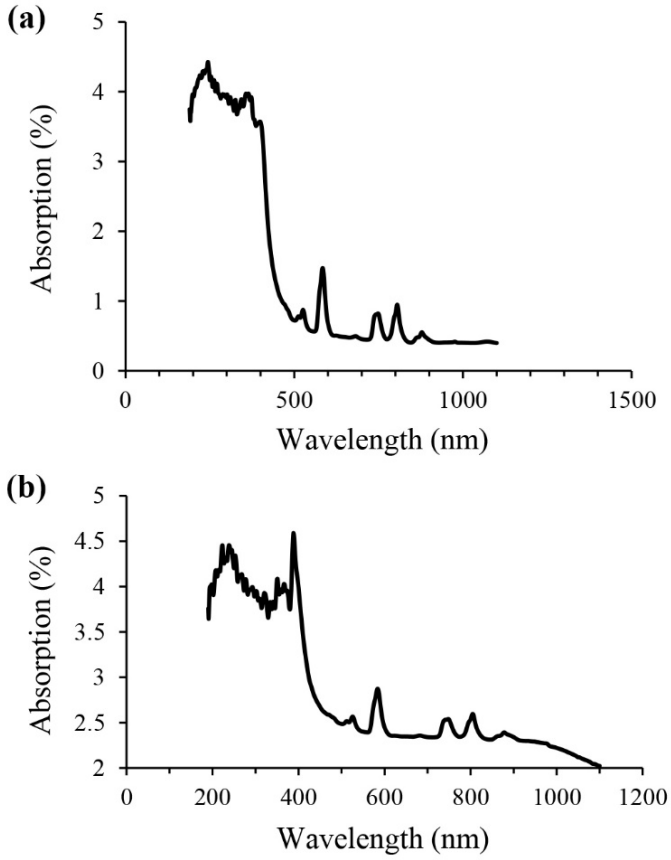

Fig. 3. a) The UV-Vis absorption spectrum of YAG composition on the base of sulfate cerium IK1 and b) the UV-Vis absorption spectrum of YAG composition on the base of IK2.

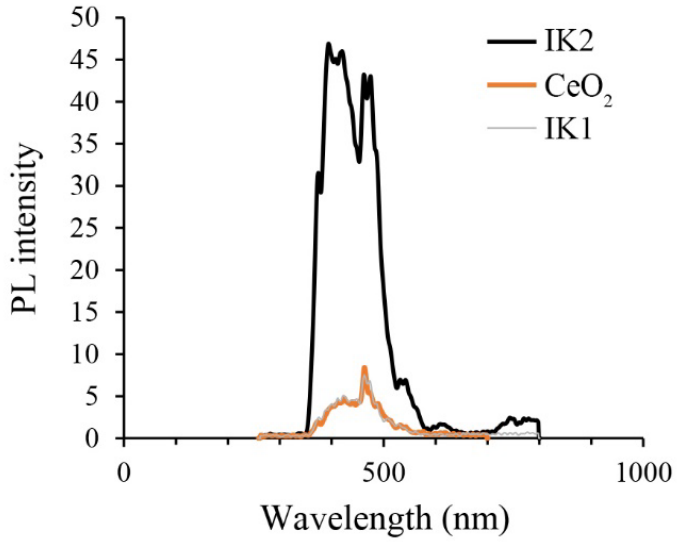

Fig. 4. The photoluminescence of YAG glasses excited by 240 nm wavelength.

also identified in the current sample. So, although the amount of neodymium oxide in the cerium sulfate sample is less than 1000 ppm, it causes the absorption spectrum in the glass in the range related to its characteristic atomic transfers. The small absorption peak at 879 nm could be related to the Yb ion formed in the glass under reducing conditions. The absorptions in the wavelength region of 260 and 320 nm are related to the absorption of cerium ions and in the wavelength range of less than 400 nm, which are presented in the curves of Fig. 2 and 3.

3.2. Evaluation of the luminance of YAG glasses

In addition to assessing the presence of cerium ions in the IK1, IK2, and CeO_2 glasses, a photoluminescence test was conducted, as demonstrated in Fig. 4. As seen in Fig. 4, the cerium oxide glass sample and IK1 have a sharp peak at the wavelength of 466 nm. Another peak with lower intensity at the wavelength of 435 nm was observed, indicating the presence of cerium ions in this glass. This peak appears to be less sharp, possibly due to the influence of ligands [25]. The emission in the IK2 sample is also in the wavelength range of 411–470 nm, which is related to transitions 4F→5D of cerium, and in general, the broad optical response of IK2 glass is in harmony with the findings of others in the wavelength range of 351 to 590 nm. However, the emission intensity, which includes two sub-emissions belonging to $^5D_1 \rightarrow {}^2F_{7/2}$ and $^5D_1 \rightarrow {}^2F_{5/2}$, is related to luminescence emission at 460 and 435 nm, respectively. The emission is more pronounced in the IK2 sample compared to the other glasses. Therefore, despite the presence of Ce^{3+} cerium ions and their characteristic energy transitions between the $^2F_{5/2}$ and $^2F_{7/2}$ states in the base state of IK2, the optical response of the material is not solely determined by cerium. Other rare earth elements, such as Yb and Nd, also contribute to the optical properties. This suggests that the optical behavior of IK2 is influenced by the combined effects of Ce^{3+} ions and other rare earth elements present in the material [24].

As can be observed in Fig. 4, emission peaks at wavelengths 400, 373, 460, and 520 nm are significant in the IK2 sample, which is probably

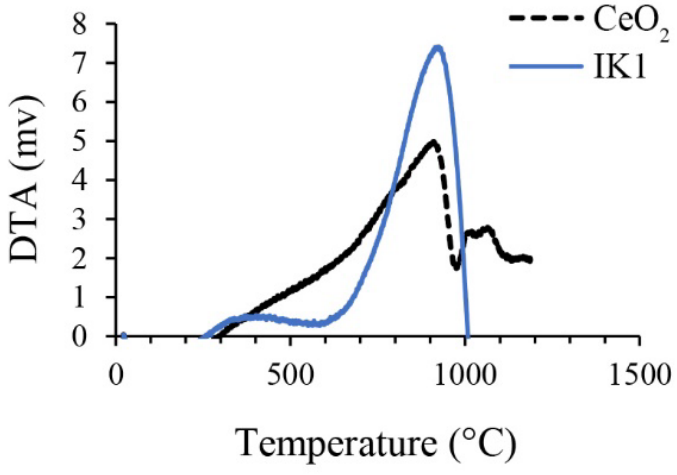

Fig. 5. DTA results of CeO_2 and IK1 glasses.

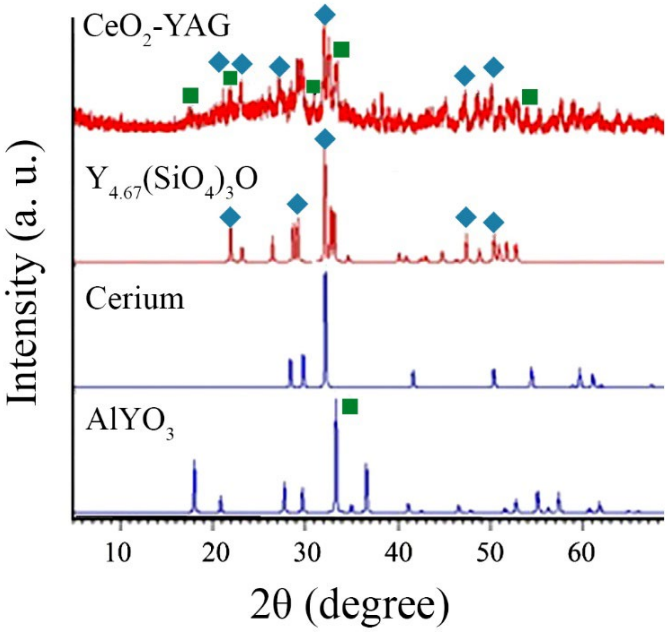

Fig. 6. XRD results of CeO_2 glasses heat treated at 1000 °C.

due to the decrease in cerium concentration and the relative increase of impurities. Optical responses at wavelengths other than 460 nm have also been detected with higher intensities. The simultaneous contamination of cerium with other rare earth elements causes a shift of the optical response to shorter wavelengths, resulting in a blue shift. It is concluded that other impurity elements, present in low concentrations along with cerium sulfate, behave as concurrent pollutants in the glass [26–28].

3.3. Thermal analysis of glass systems

A thermal analysis was conducted to compare the vitrification behavior of two glasses, IK1 and CeO_2. The results of this analysis are presented in Fig. 5. As observed, the crystallization temperature of the IK1 sample is 924 °C, while for the CeO_2 sample it is 900 °C. This indicates that the glass formability of the IK1 sample is higher compared to the CeO_2 sample. Therefore, it can be concluded that the use of cerium sulfate in glass is beneficial for enhancing glass formability. Glass formation ability has acted to the detriment of crystallization. However, with heat treatment at this temperature, all samples were amorphous, so the heat treatment time and temperature increased.

3.4. XRD results of glass ceramics heat treated at 1000 °C

All three cast and annealed glasses were heat treated at 1000 °C for 24 h and their XRD results are presented in Figs. 6, 7 and 8.

As can be seen, the glass-ceramic sample heat-treated using cerium oxide has two main phases: garnet and yttrium aluminosilicate. So garnet is crystallized in this system. However, the presence of silicate phases along with garnet is also important, which can detriment the luminosity of the garnet system.

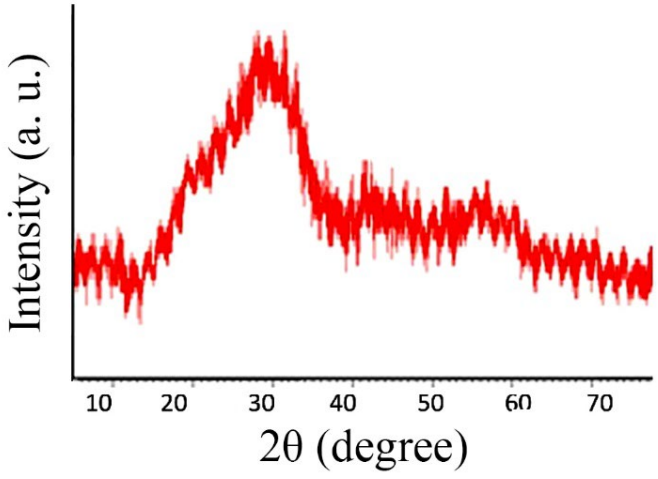

Fig. 7. XRD pattern of IK2 glasses heat treated for 24 h at 1000 °C.

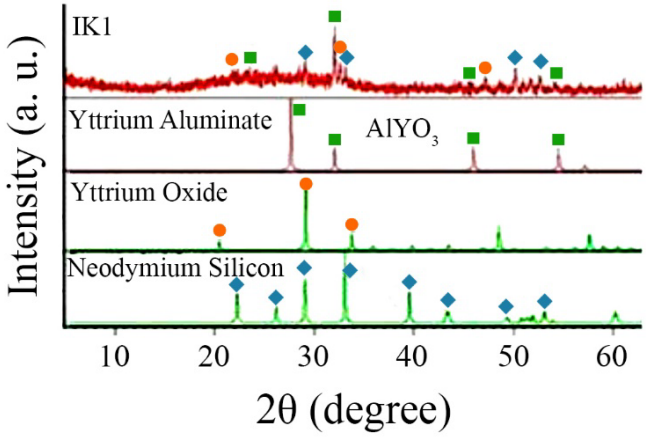

Fig. 8. XRD pattern of IK1 glasses heat treated at 1000 °C for 24 h.

According to Fig. 7, the IK2 glass sample is completely amorphous and is not crystallized. It's likely due to the smaller amount of cerium sulfate, which hasn't crystallized at this temperature. The YAG IK1 glass-ceramic sample heat treated at 1000 °C was analyzed by XRD technique. As depicted in Fig. 8, crystallization is evident in this sample. Comparing the intensity of the peaks of the main phase, it's observed that the garnet is less crystallized.

As it is clear from Fig. 9, by comparing the X-ray patterns of oxidase and sulfated samples, it can be seen that the sulfated glass sample tends to less crystallize.

3.5. Photo emission of glass ceramics

Assuming that there are silicate crystalline phases in the system, both samples were heat treated at 1060 °C for 24 h. Fig. 10 shows the results of luminescence in these three glass ceramics under excitation with wavelengths of 240 and 340 nm. IK1 glass-ceramic heat-treated at 1060 °C has a luminescence intensity at the wavelength of 460 nm, which is much higher than IK2 glass samples, the reason being the high concentration of cerium ions in the IK1 glass-ceramic structure with heat treatment. On the other hand, the light response intensity at the wavelength of 533 nm for both IK1 and IK2 glass-ceramics is higher than the corresponding glasses sample's response. Also, with excitation by 340 nm in both glass ceramics, a weak optical response at the wavelength of 420 nm is recorded.

The observation of an emission peak at 533 nm wavelength under 240 nm excitation in heat-treated glass-ceramics within the oxygen atmosphere results in the conclusion that this peak is associated with the presence of cerous ions. These ions infiltrate the garnet structure and form bonds with silica. This optical response indicates the electron dipole transfer inside cerous ions [29–32].

3.6. FT-IR evaluation

The sample prepared with one and two steps of melting by CeO_2 glass was evaluated by FT-IR technique to compare the type of bonds (Fig. 11). As can be seen, the infrared spectra of two types of glass have differences in the range of 1000 cm^{-1}, which indicates the presence of neodymium in the glass. In addition, there is no noticeable difference in the type and strength of the links. Therefore, the steps melting does not affect the type of glass bonds.

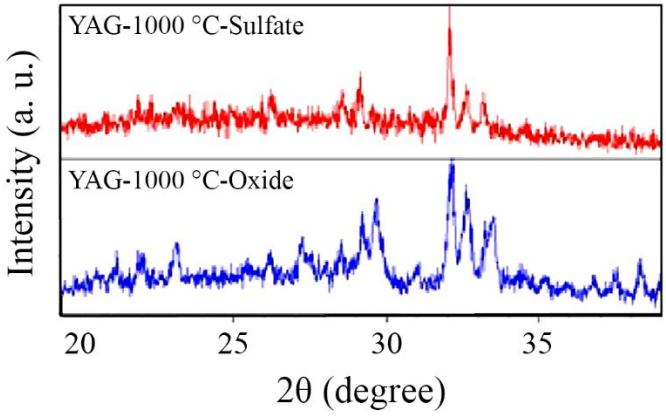

Fig. 9. Comparing XRD patterns of two YAG glasses by sulfate and oxide cerium.

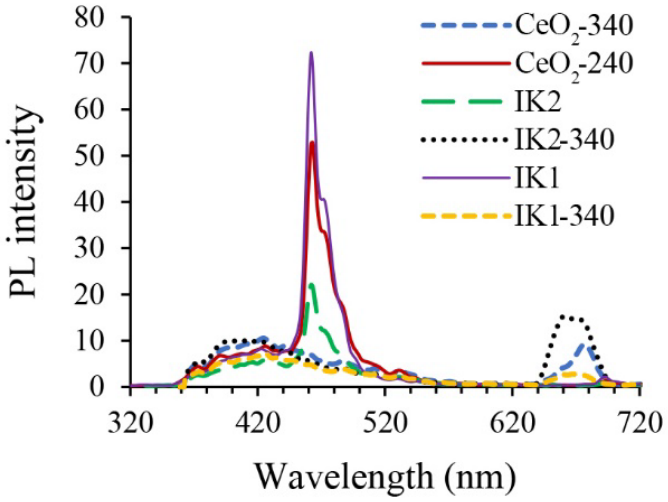

Fig. 10. The results of the luminescence of glass ceramics heat-treated at 1060 °C, excited with 240 nm with a solid line and 340 nm with a dotted line.

3.7. Luminescence of YAG glass- ceramics fabricated by SPS method

Fig. 12 shows the photoluminescence of the samples. The SPSed glass powder was mounted, polished, and evaluated for its photoluminescence properties. The samples were excited with 240 nm. The photoluminescence results are shown in Fig. 12a. In Fig. 12a, the luminescence results of the SPSed YAG glass-ceramic with a mixture of both sulfated samples using 240 nm excitation are depicted. As can be seen in Fig. 12c, despite the lower cerium content in the IK2 sample,

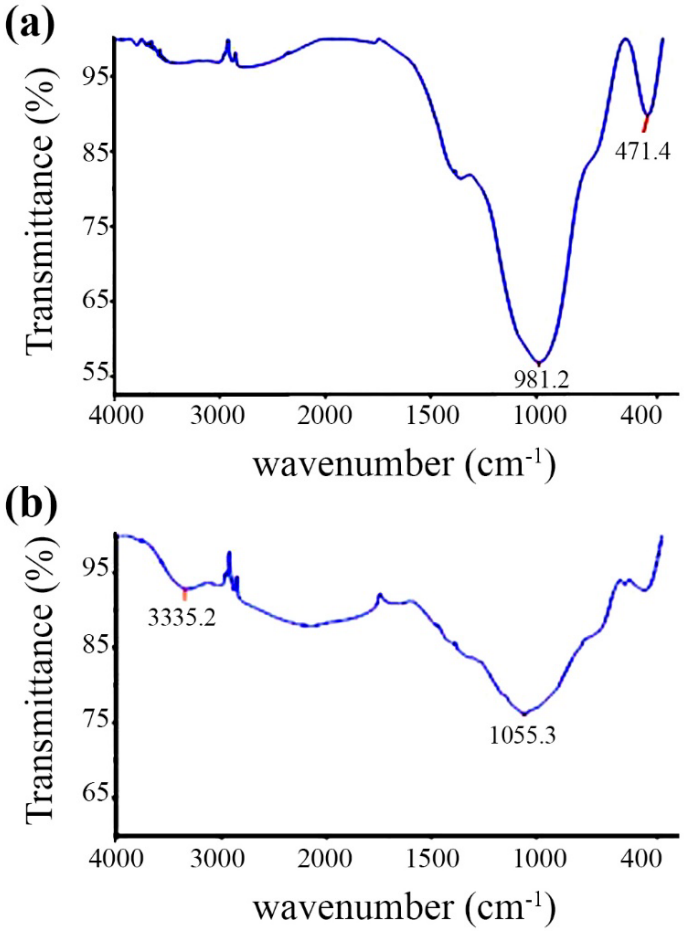

Fig. 11. a) Evaluation of cerium oxide glasses by FT-IR and b) evaluation of cerium oxide glasses by twice melting.

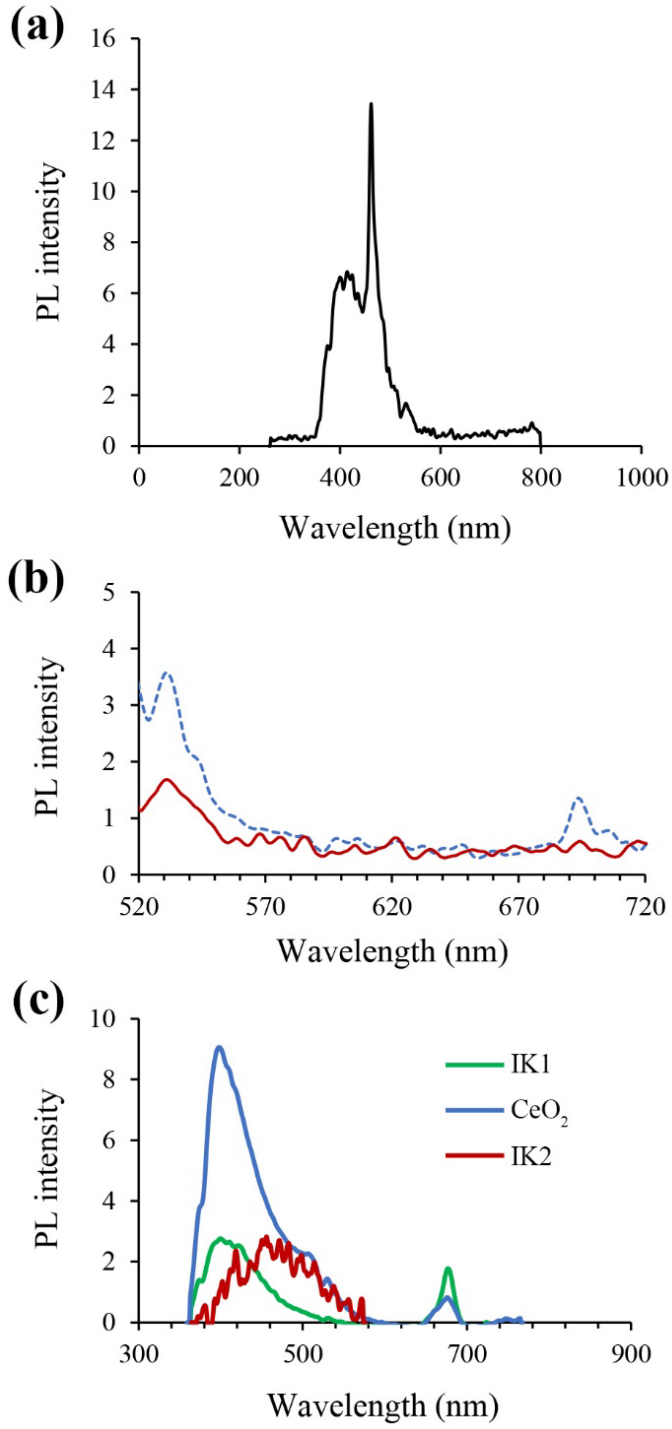

Fig. 12. Photoluminescence of SPSed YAG glass-ceramics with 240 nm wavelength excitation, b) photoluminescence of IK1, IK2 glasses heat treated at 1060 °C for 24 h, and c) photoluminescence of IK1, IK2, and CeO_2 with 2 steps heat treated at 750–1000 °C.

the two-step heat treatment intensified the luminescence properties of the YAG glass-ceramic. The peak intensity at 460 nm increased, while the peak intensity at 414 nm decreased, resulting in a sharper peak. The optical response in the range of 460 nm is related to the structure of garnet along with cerium and neodymium. However, the CeO_2 sample with heat treatment at 1060 °C has higher luminescence intensity.

It can be seen in Fig. 12b that comparing the emission intensity of the sample heat-treated using the SPS method at 1060 °C with other samples shows the remarkable effect of time during the heat treatment process for YAG glass-ceramics. Interestingly, despite this change in time, the emission wavelengths of these two samples remain consistent. However, while the SPS-synthesized sample exhibits a distinct

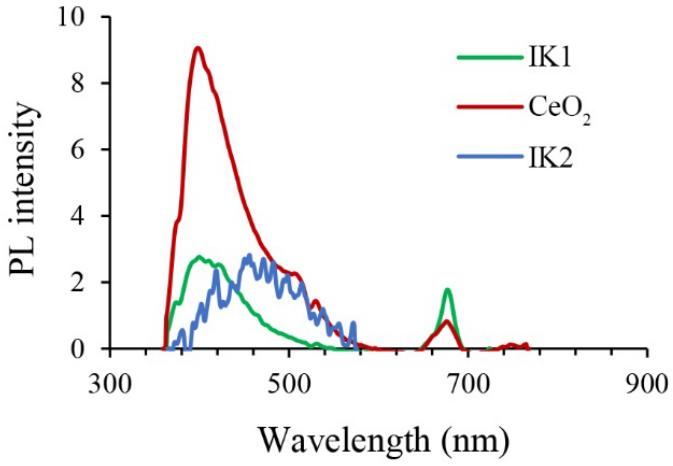

Fig. 13. Luminescence of IK1, IK2, and CeO_2 samples in two-stage heat treatment at 750–1000 °C under the atmosphere of 80% hydrogen and 20% nitrogen by excitation with 340 nm.

emission peak, its light intensity is notably lower compared to the sample heat-treated at 1060 °C for 24 h.

3.8. The luminescence of glass ceramics heat treated in hydrogen atmosphere

The luminescence results of YAG glasses IK1 and IK2 after heat treatment in a furnace under a hydrogen-nitrogen atmosphere (80% hydrogen and 20% nitrogen) in two temperature stages, first at 750 °C for 6 h, and then at 1000 °C for 12 h, are shown in Fig. 13. The results indicate a sharp peak at the wavelength of 400 nm in the CeO_2 sample, while the peaks corresponding to the wavelength of 460 nm in the IK1 and IK2 samples are less intense. These findings were obtained with 340 nm excitation. It can be concluded that the CeO_2 sample is highly sensitive to the atmosphere conditions. Moreover, based on the light response at 400 nm, it can be concluded that a significant amount of garnet is formed in this system, as garnet exhibits high reflectance at the wavelength of 400 nm [33, 34]. But the cerous ion has not penetrated inside it. Therefore, it can be said that in the case of sulfated samples, furnace atmosphere, and two-stage heat treatment did not affect the light response of garnet and cerous compared to the sample heat treated in an oxide atmosphere, and even the intensity of the light response was much less (Fig. 14). Afterward, the two-steps heat-treating in a hydrogen atmosphere of CeO_2 sample was done. It was excited with a wavelength of 460 nm, and a partial optical response was recorded in the range of 518 and 532 nm, which can be used as a supplement to yellow light in LED.

4. Conclusions

The substitution of cerium sulfate for cerium oxide in cerium-doped garnet structures has not been suggested. In this study, it was tried to lower the glass melting point by employing this combination, albeit without success. Overall, incorporating 40% mole of silica in the garnet glass composition reduces the glass's melting temperature to below 1600 °C. However, the crystallization of silicate phases negatively impacts the optical response of the garnet, particularly in the 533 nm range. In the present work, efforts were made to produce double-melted glass through heat treatment in SPS and a hydrogen atmosphere, aiming to reduce the crystallization of the silicate system. However,

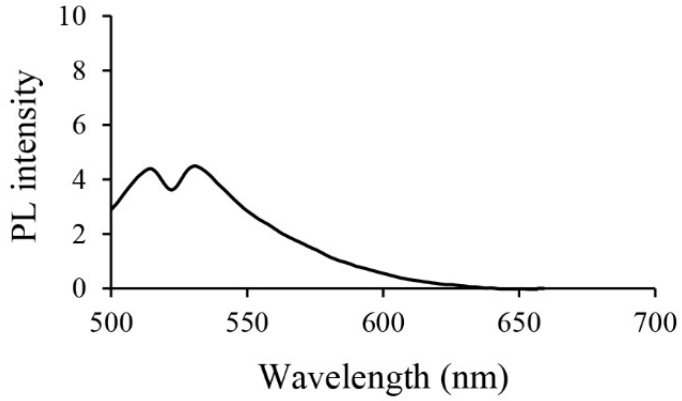

Fig. 14. The results of the luminescence of glass heat-treated in two stages with cerium oxide in a furnace with a reducing atmosphere excited with 460 nm.

based on the observed optical response of cerium ions, it was inferred that the formation of garnet structure doped with cerium ions is significantly lower in this composition compared to compounds without silica. Furthermore, the hydrogen atmosphere exhibited no discernible impact on the light response of the cerium-doped garnet structure in terms of light intensity within the 533 nm range. This suggests that the presence of SPS pressure and a reducing atmosphere did not influence the extent of crystallized garnet structure in the silicate system.

CRediT authorship contribution statement

A. Faeghinia: Conceptualization, Funding acquisition, Investigation, Writing – original draft, Writing – review & editing.

Data availability

The data underlying this article will be shared on reasonable request to the corresponding author.

Declaration of competing interest

The author declares no competing interests.

Funding and acknowledgment

The author gratefully acknowledges the generous support provided by the Materials and Energy Research Center, under the M. S. Project with Contract No. 223530001. This study was also financially supported by the Materials and Energy Research Center through Grant No. 371398055.

References

[1] A. Faeghinia, Impact of bridging oxygens formation on optical properties of Fe3+ doped Li2O–Al2O3–SiO2–TiO2 glasses, Synth. Sinter. 2 (2022) 14–19. https://doi.org/10.53063/synsint.2022.2179.

[2] X. Sun, J. Wen, Q. Guo, F. Pang, Z. Chen, et al., Fluorescence properties and energy level structure of Ce-doped silica fiber materials, Opt. Mater. Express. 7 (2017) 751. https://doi.org/10.1364/OME.7.000751.

[3] H. Hua, S. Feng, Z. Ouyang, H. Shao, H. Qin, et al., YAGG:Ce transparent ceramics with high luminous efficiency for solid-state lighting application, J. Adv. Ceram. 8 (2019) 389–398. https://doi.org/10.1007/s40145-019-0321-9.

[4] N.K. Giri, N. Agnihotri, R. Prakash, Ceramic-based upconversion phosphors, in: Upconversion Nanophosphors, Elsevier. (2022) 181–202. https://doi.org/10.1016/B978-0-12-822842-5.00008-X.

[5] I. Ahemen, K.D. Dilip, A.N. Amah, A review of solid state white light emitting diode and its potentials for replacing conventional lighting technologies in developing countries, Appl. Phys. Res. 6 (2014) 95–108. https://doi.org/10.5539/apr.v6n2p95.

[6] Y. Pan, M. Wu, Q. Su, Comparative investigation on synthesis and photoluminescence of YAG:Ce phosphor, Mater. Sci. Eng. B. 106 (2004) 251–256. https://doi.org/10.1016/j.mseb.2003.09.031.

[7] M. Gong, X. Liang, Y. Wang, H. Xu, L. Zhang, W. Xiang, Novel synthesis and optical characterization of phosphor-converted WLED employing Ce:YAG-doped glass, J. Alloys Compd. 664 (2016) 125–132. https://doi.org/10.1016/j.jallcom.2015.12.239.

[8] Y. Zhuang, C. Li, C. Liu, Y. Fu, Q. Shi, et al., High-efficiency YAG:Ce3+ glass-ceramic phosphor by an organic-free screen-printing technique for high-power WLEDs, Opt. Mater. (Amst). 107 (2020) 110118. https://doi.org/10.1016/j.optmat.2020.110118.

[9] M. Jia, J. Wen, W. Luo, Y. Dong, F. Pang, et al., Improved scintillating properties in Ce:YAG derived silica fiber with the reduction from Ce4+ to Ce3+ ions, J. Lumin. 221 (2020) 117063. https://doi.org/10.1016/j.jlumin.2020.117063.

[10] J. Kalahe, M.P. Stone, P.D. Dragic, J. Ballato, J. Du, The structures and properties of yttrium aluminosilicate glasses with low, medium, and high silica contents, J. Non. Cryst. Solids. 614 (2023) 122394. https://doi.org/10.1016/j.jnoncrysol.2023.122394.

[11] X. He, X. Liu, R. Li, B. Yang, K. Yu, et al., Effects of local structure of Ce3+ ions on luminescent properties of Y3Al5O12:Ce nanoparticles, Sci. Rep. 6 (2016) 22238. https://doi.org/10.1038/srep22238.

[12] D.Y. Kosyanov, X. Liu, A.A. Vornovskikh, A.P. Zavjalov, A.M. Zakharenko, et al., Al2O3–Ce:YAG composite ceramics for high brightness lighting: Cerium doping effect, J. Alloys Compd. 887 (2021) 161486. https://doi.org/10.1016/j.jallcom.2021.161486.

[13] R. Marin, G. Sponchia, P. Riello, R. Sulcis, F. Enrichi, Photoluminescence properties of YAG:Ce3+,Pr3+ phosphors synthesized via the Pechini method for white LEDs, J. Nanoparticle Res. 14 (2012) 886. https://doi.org/10.1007/s11051-012-0886-5.

[14] L. Wang, L. Mei, G. He, G. Liu, J. Li, L. Xu, Crystallization and fluorescence properties of Ce:YAG glass-ceramics with low SiO2 content, J. Lumin. 136 (2013) 378–382. https://doi.org/10.1016/j.jlumin.2012.12.019.

[15] L. Wang, L. Mei, G. He, J. Li, L. Xu, Preparation of Ce:YAG Glass-Ceramics with Low SiO2, J. Am. Ceram. Soc. 94 (2011) 3800–3803. https://doi.org/10.1111/j.1551-2916.2011.04700.x.

[16] S.F. Wang, J. Zhang, D.W. Luo, F. Gu, D.Y. Tang, et al., Transparent ceramics: Processing, materials and applications, Prog. Solid State Chem. 41 (2013) 20–54. https://doi.org/10.1016/j.progsolidstchem.2012.12.002.

[17] E.H. Penilla, Y. Kodera, J.E. Garay, Simultaneous synthesis and densification of transparent, photoluminescent polycrystalline YAG by current activated pressure assisted densification (CAPAD), Mater. Sci. Eng. B. 177 (2012) 1178–1187. https://doi.org/10.1016/j.mseb.2012.05.026.

[18] A. Faeghinia, H. Nuranian, M. Eslami, Synthesis of magnetite-silica-carbon quantum dot nanocomposites for melatonin drug delivery, Synth. Sinter. 3 (2023) 79–87. https://doi.org/10.53063/synsint.2023.32142.

[19] V.D. Paygin, A.E. Ilela, D.E. Deulina, G. V Lyamina, S.A. Stepanov, et al., Spark plasma sintering of transparent YAG:Ce ceramics with LiF flux, J. Phys. Conf. Ser. 1989 (2021) 012008. https://doi.org/10.1088/1742-6596/1989/1/012008.

[20] B. Priyadarshini, U. Anjaneyulu, U. Vijayalakshmi, Preparation and characterization of sol-gel derived Ce4+ doped hydroxyapatite and its in vitro biological evaluations for orthopedic applications, Mater. Des. 119 (2017) 446–455. https://doi.org/10.1016/j.matdes.2017.01.095.

[21] M. Cieslikiewicz-Bouet, H. El Hamzaoui, Y. Ouerdane, R. Mahiou, G. Chadeyron, et al., Investigation of the incorporation of cerium ions in MCVD-silica glass preforms for remote optical fiber radiation dosimetry, Sensors. 21 (2021) 3362. https://doi.org/10.3390/s21103362.

[22] R. Zhou, C. Calahoo, Y. Ding, L. Wondraczek, Role of Ag+ ions in determining Ce3+ optical properties in fluorophosphate and sulfophosphate glasses, ACS Omega. 6 (2021) 30093–30107. https://doi.org/10.1021/acsomega.1c04933.

[23] W.W. Wendlandt, The thermal decomposition of yttrium and the rare earth metal sulphate hydrates, J. Inorg. Nucl. Chem. 7 (1958) 51–54. https://doi.org/10.1016/0022-1902(58)80026-3.

[24] U. Berwal, V. Singh, R. Sharma, Effect of Ce4+→Ce3+ conversion on the structural and luminescence properties of Ce4+ doped Gd2Ti2O7 pyrochlore oxide, J. Lumin. 257 (2023) 119687. https://doi.org/10.1016/j.jlumin.2023.119687.

[25] H. Tagawa, Thermal decomposition temperatures of metal sulfates, Thermochim. Acta. 80 (1984) 23–33. https://doi.org/10.1016/0040-6031(84)87181-6.
[26] E. Allahkarami, B. Rezai, A literature review of cerium recovery from different aqueous solutions, J. Environ. Chem. Eng. 9 (2021) 104956. https://doi.org/10.1016/j.jece.2020.104956.
[27] A. Yusuf, A. Giwa, J.O. Eniola, H.K. Amusa, M.R. Bilad, Recent advances in catalytic sulfate radical-based approach for removal of emerging contaminants, J. Hazard. Mater. Adv. 7 (2022) 100108. https://doi.org/10.1016/j.hazadv.2022.100108.
[28] P. Meshram, Abhilash, Recovery and recycling of cerium from primary and secondary resources- a critical review, Miner. Process. Extr. Metall. Rev. 41 (2020) 279–310. https://doi.org/10.1080/08827508.2019.1677647.
[29] J.F. Olorunyomi, J.F. White, T.R. Gengenbach, R.A. Caruso, C.M. Doherty, Fabrication of a reusable carbon dot/gold nanoparticle/metal–organic framework film for fluorescence detection of lead ions in water, ACS Appl. Mater. Interfaces. 14 (2022) 35755–35768. https://doi.org/10.1021/acsami.2c09122.
[30] S. Foteinopoulou, G.C.R. Devarapu, G.S. Subramania, S. Krishna, D. Wasserman, Phonon-polaritonics: enabling powerful capabilities for infrared photonics, Nanophotonics. 8 (2019) 2129–2175. https://doi.org/10.1515/nanoph-2019-0232.
[31] B.M. Walsh, N.P. Barnes, D.J. Reichle, S. Jiang, Optical properties of Tm3+ ions in alkali germanate glass, J. Non. Cryst. Solids. 352 (2006) 5344–5352. https://doi.org/10.1016/j.jnoncrysol.2006.08.029.
[32] V. Tucureanu, A. Matei, A.M. Avram, Synthesis and characterization of YAG:Ce phosphors for white LEDs, Opto-Electron. Rev. 23 (2015) 239–251. https://doi.org/10.1515/oere-2015-0038.
[33] Z. Song, C. Kuenzer, Spectral reflectance (400–2500 nm) properties of coals, adjacent sediments, metamorphic and pyrometamorphic rocks in coal-fire areas: A case study of Wuda coalfield and its surrounding areas, northern China, Int. J. Coal Geol. 171 (2017) 142–152. https://doi.org/10.1016/j.coal.2017.01.008.
[34] J. Liang, B. Devakumar, L. Sun, S. Wang, Q. Sun, X. Huang, Full-visible-spectrum lighting enabled by an excellent cyan-emitting garnet phosphor, J. Mater. Chem. C. 8 (2020) 4934–4943. https://doi.org/10.1039/D0TC00006J.